The improved multi-criteria decision-making model for multi-objective operation in a complex reservoir system

Zhe Yang, Kan Yang, Yufeng Wang, Lyuwen Su and Hu Hu

ABSTRACT

In multi-objective reservoir operation, it is vital for decision-makers to select optimal scheduling schemes through efficient multi-criteria decision-making (MCDM) techniques. However, in the family of MCDM methods, it is difficult for the technique for order preference by similarity to an ideal solution (TOPSIS) to describe grey correlation, thus making decisions with less reliability. To this end, a framework supporting high-quality solutions' acquirement and optimal reservoir operation decision-making is established. The improved multi-objective particle swarm optimization (IMOPSO), a new efficient MCDM model based on TOPSIS and grey correlation analysis (GCA), and combination weighting method based on the minimum deviation (CWMMD) are included in the framework. The non-inferior solution set is efficiently obtained by IMOPSO and optimal decision information is provided for decision-makers using the MCDM model. Moreover, the CWMMD is used to determine weighting information of multiple evaluation indicators. Numerical simulations are conducted to verify the efficiency of the proposed methodology and support decision-making for multi-objective reservoir operation in Hongjiadu and Qingjiang basins. The results indicate that the proposed methodology can provide non-inferior scheduling solutions and decision-making instruction with higher reliability for multi-objective reservoir operation.

Key words | combination weighting method based on the minimum deviation (CWMMD), grey correlation analysis (GCA), improved multi-objective particle swarm optimization (IMOPSO), multi-criteria decision-making (MCDM), multi-objective reservoir operation, TOPSIS

Zhe Yang
Kan Yang (corresponding author)
Lyuwen Su
Hu Hu
College of Hydrology and Water Resources,
Hohai University,
Nanjing, Jiangsu 210098,
China
E-mail: *kyang@hhu.edu.cn*

Zhe Yang
IIHR-Hydroscience and Engineering,
University of Iowa, C. Maxwell Stanley Hydraulics Laboratory,
Iowa City, IA,
USA

Yufeng Wang
School of Water Resources and Environment,
China University of Geosciences (Beijing),
Beijing 100083,
China

INTRODUCTION

Complex reservoir systems, especially cascade reservoirs, are built to control flood control and increase social, economic, and ecological benefits. Optimal reservoir operation requires simultaneous optimization of multiple competing objectives, such as hydropower generation, flood control, safety requirements of upstream and downstream regions, the water supply and shipping (Jia *et al.* 2016). Due to the multiple benefits of optimization, it is unpractical to find a single scheduling scheme to balance all the objectives. Instead, solutions with trade-offs, also referred to as Pareto optimal solutions are selected by decision-makers, and thus, multi-objective reservoir operation can be defined as a multi-criteria decision-making (MCDM) problem (Zhu *et al.* 2016, 2017). As a group of satisfying solutions are provided to decision-makers, they need to locate the most ideal or comprehensive solution to operate a reservoir. To this end, it is of great theoretical and practical significance to develop an effective MCDM method to rank Pareto optimal solutions.

TOPSIS refers to the technique for order performance by similarity to ideal solution which is a classical MCDM method proposed to rank various schemes according to

doi: 10.2166/hydro.2019.150

closeness to the ideal alternative (Hwang & Yoon 1981). Based on the concept of ideal and anti-ideal point, the most satisfying alternative obtained by the TOPSIS method is defined as the alternative that is simultaneously closest to the ideal alternative and farthest from the anti-ideal alternative. TOPSIS has been widely applied to solve MCDM problems and recommended by the United Nation Environmental Program (Abo-Sinna *et al.* 2008; Afshar *et al.* 2011). Meanwhile, improvements to TOPSIS have also received deserved attention. Yu *et al.* (2004) proposed an improved TOPSIS based on the fuzzy preference. Karimi *et al.* (2012) extended the traditional TOPSIS method to fuzzy TOPSIS method and applied it to financial risk management. Wang & Wang (2014) and Chen & Lu (2015) replaced Euclid distance with the Mahalanobis distance to modify conventional TOPSIS and combined it with fuzzy analytical hierarchy process (FAHP). Deng *et al.* (2000) attempted to improve TOPSIS from the aspect of scientific indicator or criterion weights' determination.

However, due to the limitations of cognitive ability and complexity of evaluation object, information such as attribute or preference is missing in many decision-making problems and cannot be completely represented by certain values. For an MCDM problem of multi-objective reservoir operation, it is a complicated decision-making process to evaluate and optimize the comprehensive reservoir operation schemes. In addition, as multi-objective reservoir operation is not limited to a single reservoir, cascade reservoirs are jointly operated in order to maximize overall benefit (Wang *et al.* 2014; Li & Ouyang 2015; Peng *et al.* 2015). In comparison with a single reservoir, the MCDM problem of complex cascade reservoir systems is more challenging and complex because more hydraulic constraints, uncertainty factors, and decision criteria should be considered for assessing the quality of scheduling schemes. Furthermore, the hidden interrelation and coupling relation among the indicators and criteria make the reservoir operation scheme reveal the inner grey correlation. The grey correlation also referred to as 'grey characteristics' between evaluation indicators cannot be described or solved by TOPSIS. To this end, grey correlation analysis (GCA) is combined with TOPSIS to efficiently show the inner correlation between scheduling schemes.

The GCA is derived from grey system theory proposed to solve the problem of incomplete information and uncertain system. It is also a family of MCDM methods for assisting the decision process in multi-criteria or attribute system. GCA describes the similarity of factors according to the closeness of variation trend among factors, and its essence is to judge the correlation degree of data according to the similarity degree of geometric relationship between data (Jiang *et al.* 2007). Therefore, GCA has become a common mathematical tool in the field of MCDM. Zeng *et al.* (2003) established a multi-objective decision model based on grey relational analysis and applied it to the optimization of normal reservoir water level. Li *et al.* (2009) applied a grey relational analysis model based on improved entropy weight to optimize the evaluation of reservoir scheduling schemes.

In this paper, we proposed an improved MCDM method based on GCA and TOPSIS dealing with optimization of scheduling scheme for multi-criteria flood control operation and multi-objective ecological and water supply operation in complex reservoir systems. The weights of indicators or multiple criteria are determined using combination weighting method based on minimum deviation (CWMMD). In recent years, single objective and multi-objective optimization techniques have been widely used to solve optimization problems including reservoir operation (Azamathulla *et al.* 2008; He *et al.* 2014; Luo *et al.* 2015; Jia *et al.* 2016; Shi *et al.* 2017; Yang *et al.* 2019a, 2019b, 2019c). As a family of multi-objective optimization methods, MOPSO and modified versions have been widely used to solve multi-objective optimization problems and received deserved attention (Dai *et al.* 2015; Li *et al.* 2016; Sheikholeslami & Navimipour 2017; Laskar *et al.* 2018; Zain *et al.* 2018). To efficiently solve the multi-objective optimization model and obtain non-inferior solutions, we proposed effective improvements based on conventional MOPSO. Thereafter, the ranking order of all the feasible scheduling schemes or alternatives can be obtained using the GCA-TOPSIS proposed. Finally, we apply the proposed methodologies to decision-making for flood control operation in Hongjiadu reservoir, and ecological and water supply operation in Qingjiang cascade reservoirs. The results show that the proposed methodology can effectively locate the ideal reservoir scheduling information for decision-makers and

improve the reliability of decisions for multi-objective reservoir operation with emphasis on flood control, ecology, and water supply.

THE IMPROVED MCDM MODEL BASED ON GCA-TOPSIS

Definition of MCDM problem

As a large-scale water control system with multiple objectives, reservoir operation usually has multiple functions such as flood control, power generation, shipping, and water supply. Due to the presence of the multiple objectives, it is difficult to find a single optimal solution that optimizes all goals. Instead, multiple solutions exist in the form of trade-offs, also referred to as Pareto optimal solutions (Malekmohammadi *et al.* 2011). We use MCDM methods to evaluate and select the most preferred solution from the set of non-inferior solutions on the Pareto front for decision-makers (Zhu *et al.* 2017). In general, an MCDM problem consists of a set of alternatives, criteria, and an MCDM model. In terms of this study, the non-inferior solutions are viewed as alternatives. The criteria are related to the function of reservoirs and weighting information is decided by CWMMD. For the MCDM model, we proposed a decision-making method on the basis of GCA and TOPSIS.

The description of GCA

Grey correlation analysis is a method to determine the quality grade of samples according to the correlation between the comparison sequence and the reference sequence. The reference sequence has the best correlation with the largest degree of correlation, and the quality grade of the sample can be obtained accordingly. The principle of GCA is simple and requires fewer original data with more convenient operation (Zhang & Liang 2009). These features make it easier to mine data rules. The essential steps of a GCA model include: (1) data sequence determination including reference and comparison sequences, (2) building a decision matrix, (3) calculating ideal and anti-ideal schemes, (4) calculating correlation coefficient and correlation degree. The higher the correlation degree is, the better the scheme will be.

The grey correlation coefficient (GCC) is defined as:

$$\begin{cases} \varsigma_{0i}(j) = \dfrac{\mu + \rho\eta}{\Delta_i(j) + \rho\eta} \\ \eta = \max\limits_i \max\limits_j \Delta_i(i) \\ \mu = \min\limits_i \min\limits_j \Delta_i(i) \\ \Delta_i(j) = |x_0(j) - x_i(j)| \end{cases} \tag{1}$$

where $\varsigma_{0i}(j)$ is the grey correlation coefficient; $\Delta_i(j)$ is difference sequence; $x_0(j)$ denotes the ideal solution in terms of the jth indicator; $x_i(j)$ is the ith solution in terms of the jth indicator; η and μ = maximum and minimum difference in difference sequence, respectively; and ρ denotes identification coefficient which is distributed in the range of [0,1].

The grey correlation degree (GCD) can be calculated by the following equation:

$$r_i = \sum_{i=1}^{m} weight_j^T \varsigma_{0i}(j) \tag{2}$$

where r_i is grey correlation degree of the ith evaluation schemes with weighting; $weight_j^T$ is the weight of the jth indicator.

Due to less strict quantitative requirements for data and simple calculation, GCA is widely used in fields such as social science, decision-making, and management. In practice, GCA is capable of analyzing the correlation between the same elements in different schemes; however, it is impossible to compare the close degree of different elements.

The TOPSIS model

TOPSIS is a well-known MCDM method based on the concept of ideal and anti-ideal points, where the best alternative should be the one that is closest to the ideal alternative and farthest from the anti-ideal alternative (Hwang & Yoon 1981). This method has no strict restrictions and requirements in terms of the number of indicators, also referred to as criteria, samples, and data. It can fully make use of original data with less information loss (Lei *et al.* 2016).

The main advantages of TOPSIS include: (1) its robust logical structure, (2) its powerful computation capability, and (3) its ability to consider ideal and anti-ideal points simultaneously. The main steps of TOPSIS can be elaborated as follows.

Step (1): Building a normalized decision matrix and calculating the corresponding weighted matrix. The normalization and weighted methods are as follows:

$$\begin{cases} nor_{ij} = \dfrac{\max_{ij} - x_{ij}}{\max_{ij} - \min_{ij}} & \text{For the benefit type indicator} \\ nor_{ij} = \dfrac{x_{ij} - \min_{ij}}{\max_{ij} - \min_{ij}} & \text{For the cost type indicator} \end{cases} \tag{3}$$

$$Wv = (v_{ij})_{m\times n} = v_{ij} = \omega_i x_{ij}, i, j \in m, n \tag{4}$$

where x_{ij} is the initial value of the jth indicator in the ith evaluation schemes; v_{ij} is the weighted x_{ij}; nor_{ij} is the value with normalization; $\max_{ij}$ and $\min_{ij}$ are maximum and minimum value of the jth indicator in the ith evaluation schemes.

Step (2): Calculate ideal and anti-ideal solutions according to the following principle:

$$\begin{cases} v_i^+ = \{v_1^+, v_2^+, \ldots\ldots\ldots\ldots v_n^+\} \\ \quad = \{(\max v_{ij} | j \in Ben), (\min v_{ij} | j \in Cost)\} \\ v_i^- = \{v_1^-, v_2^-, \ldots\ldots\ldots\ldots v_n^-\} \\ \quad = \{(\max v_{ij} | j \in Ben), (\min v_{ij} | j \in Cost)\} \end{cases} \tag{5}$$

where v_i^+ and v_i^- are ideal and anti-ideal solutions, respectively.

Step (3): Calculate the Euclidean distance (ED) between the value of each indicator and the ideal and anti-ideal solutions (D_i^+ and D_i^-). The specific method is shown as follows:

$$\begin{cases} D_i^+ = \sqrt{\sum_{j=1}^{n} (v_{ij} - v_j^+)^2} \\ D_i^- = \sqrt{\sum_{j=1}^{n} (v_{ij} - v_j^-)^2} \end{cases} \tag{6}$$

Step (4): Calculate close degree $Close_i$ which represents the degree of proximity between each scheme and the optimal one. The closeness is described by the following equation:

$$Close_i = \frac{D_i^-}{D_i^+ + D_i^-} \tag{7}$$

The TOPSIS also has defects including: (1) when calculating the distance between the evaluation object and ideal and anti-ideal solutions, the correlation between indicators cannot be fully considered; (2) the schemes may be equally close to the ideal and anti-ideal solutions, making it impossible to locate the best scheme.

The GCA-TOPSIS model

Multi-objective reservoir operation including objectives such as flood control, ecological, power generation, and water supply is affected by the uncertainty of hydrology, hydraulics, and reservoir operation management. These uncertain factors have great influence on the scheduling decision, which may lead to differences between the actual scheduling process and the scheduling scheme made under certain conditions. In the decision-making process of multi-objective reservoir operation, due to uncertainty factors, insufficient statistical data, great data fluctuation, and inapparent typical distribution rule, the uncertainty of quantitative relationship between evaluation criteria will lead to obvious 'grey characteristics'. To this end, in terms of potential defects existing in GCA and TOPSIS, we build a decision-making model coupling the GCA and TOPSIS to make full utilization of their respective strengths. The GCA contributes to reflecting the difference between the change trend in scheduling scheme sets and ideal scheme, and places emphasis on the internal connection between indicators. Meanwhile, the TOPSIS can reflect the overall similarity between alternative and ideal schemes. The combination of GCA and TOPSIS makes the decision-making for multi-objective reservoir operation more scientific and reasonable. The coupling process is elaborated as follows.

Step (1): Assuming that the solution set for reservoir multi-objective operation is $S = \{S_1, S_2, \ldots\ldots\ldots\ldots S_n\}$; the solution decision matrix is $x_{ij} = [x_{i1}, x_{i2}, \ldots\ldots\ldots\ldots x_{in}]$ $i = 1, 2 \ldots..m; j = 1, 1 \ldots..n$; the weighting vector is $\omega = (\omega_1, \omega_2 \ldots..\omega_n)$; the corresponding weighted solution decision matrix is $v_{ij} = [v_{i1}, v_{i2}, \ldots\ldots\ldots\ldots v_{in}]$.

Step (2): Normalize the initial decision matrix x_{ij} and calculate v_{ij} according to methods mentioned in the section 'The TOPSIS model'.

Step (3): Determine the ideal and anti-ideal solutions of v_{ij} according to **Step (2)** in the section 'The TOPSIS model'.

Step (4): Calculate the ED between each scheme and the ideal and anti-ideal solutions (D_j^+ and D_j^-) in accordance with Step (3).

Step (5): Calculate the grey correlation coefficient (GCC) matrix between each scheme and the ideal and anti-ideal solution (ς^+ and ς^-) according to the following equation:

$$\begin{cases} \varsigma^+ = (\varsigma_{ij}^+)_{m\times n}, \varsigma^- = (\varsigma_{ij}^-)_{m\times n} \\ \varsigma_{ij}^+ = \dfrac{\min\left|v_j^+ - v_{ij}\right| + \rho\max\left|v_j^+ - v_{ij}\right|}{\left|v_j^+ - v_{ij}\right| + \rho\max\left|v_j^+ - v_{ij}\right|} \\ \varsigma_{ij}^- = \dfrac{\min\left|v_j^- - v_{ij}\right| + \rho\max\left|v_j^- - v_{ij}\right|}{\left|v_j^- - v_{ij}\right| + \rho\max\left|v_j^- - v_{ij}\right|} \end{cases} \tag{8}$$

where ς_{ij}^+ and ς_{ij}^- are correlation coefficient elements in the matrix; ρ, v_i^+, v_i^- and v_{ij} are in line with the above. The empirical value of ρ is 0.5 usually.

Step (6): The corresponding grey correlation degree (GCD) matrix (r_i^+ and r_i^-) is obtained according to the following equation:

$$\begin{aligned} r_i^+ &= \sum_{i=1}^{m} weight_i^T \varsigma_{ij}^+ \\ r_i^- &= \sum_{i=1}^{m} weight_i^T \varsigma_{ij}^- \end{aligned} \tag{9}$$

Step (7): The ED and GCD are merged after dimensionless treatment. The merge equations can be determined as follows:

$$\begin{cases} TOP_i^+ = \dfrac{D_i^+}{D_i^+ + D_i^-} \\ GCA_i^+ = \dfrac{R_i^+}{R_i^+ + R_i^-} \end{cases} \tag{10}$$

where TOP_i^+ and GCA_i^+ are merge equations; D_i^+ and D_i^- are ED with dimensionless treatment; R_i^+ and R_i^- are GCD with dimensionless treatment. The higher the value of D_i^- and R_i^+ is, the better the feasible scheme will be. On the contrary, the lower the value of D_i^+ and R_i^- is, the better the feasible scheme will be.

Step (8): The relative similarity degree C_i^* is defined to reflect the closeness degree of the feasible scheme to the ideal or anti-ideal scheme in terms of situation change. The higher the value is, the better the scheme will be and vice versa. The relative similarity degree can be calculated according to the following equation:

$$\begin{cases} C_i^* = \alpha_1 TOP_i^+ + \alpha_2 GCA_i^+ \\ \alpha_1 + \alpha_2 = 1 \quad \alpha_1, \alpha_2 \in (0, 1) \end{cases} \tag{11}$$

where α_1 and α_2 denote preference degree of the decision-maker. Normally, the values of α_1 and α_2 are consistent.

THE COMBINATION WEIGHTING METHOD BASED ON MINIMUM DEVIATION

It is critical to confirm indicator weights in order to quantitatively describe the importance for evaluation indicators and improve reliability of evaluation results. To our knowledge, weighting methods can be divided into two types: subjective and objective measures. The former is to determine the indicator weight according to the subjective indicator emphasis. The latter obtains the weight from original objective information of indicators. To take advantage of the two types of weighting methods, the combination weighting method is used to achieve balance between subjective intention and objectivity of indicator.

Normally, combination weights are calculated by linear combination coefficient which is subjected to subjective experiences. Therefore, in this work, combination weighting measure based on minimum deviation is proposed to get the optimal weight combination. The analytic hierarchy process (AHP) and improved entropy method are selected as the subjective and objective weighting measure, respectively. The details of AHP and improvements for entropy method can be seen in research by Yang *et al.* (2019a).

The improved entropy weight method

In terms of conventional entropy method, the entropy coefficient E_i and entropy weight ω_i corresponding to the indicator i are calculated according to the following equations:

$$\begin{cases} E_i = -k \sum_{j=1}^{m} x_{ij} \ln x_{ij} \\ k = \ln n \end{cases} \tag{12}$$

$$\omega_i = \frac{(1 - E_i)}{(n - \sum_{i=1}^{n} E_i)}, \; 0 \le \omega_i \le 1 \tag{13}$$

where k is standard coefficient; n denotes indicator amount; m represents observed sample data of evaluation indicators; and x_{ij} is the jth standardized sample date of the indicator i.

The nature of entropy includes: (1) If the entropy value of an indicator is large, it indicates that the value difference of each scheme on this indicator is small. The corresponding value of entropy weight ω_i is also small and vice versa. (2) If all schemes have the same value of one indicator, the entropy value of this indicator E_i is assumed to be $(1(E_i = 1))$.

For the conventional entropy method, the small changes of E_i will bring about a tremendous margin of indicator entropy weight ω_i, especially when $E_i \to 1$. For this purpose, the entropy equation is modified as follows:

$$\begin{cases} \omega_i = \dfrac{(1 - E_i)}{\sum_{i=1}^{n} (1 - E_i)} \left(1 - \bar{E}\right) + \dfrac{(1 + \bar{E} - E_i)}{\sum_{i=1, E_i \ne 1}^{n} (1 + \bar{E} - E_i)} \bar{E} & E_i < 1 \\ \omega_i = 0 & E_i = 1 \end{cases} \tag{14}$$

where $\bar{E}$ is the mean of entropy coefficient; ω_i denotes the weight of ith indicator.

To verify the reasonability of the improved entropy weight method, comparison between it and conventional entropy method is displayed in Table 1.

From the results in Table 1, indicator weights obtained by the improved entropy method are more reasonable in terms of distribution circumstance 1. The indicator weight is distributed more evenly with small changes of E_i. When the weights present discrete distribution, results of the improved method coincide with the conventional one as well. Therefore, the indicator weights calculated by the improved entropy method are more objective and reliable than that of the conventional one.

Weight combination based on minimum deviation principle (CWMMD)

Assume that total r weight determination methods are selected, and m represents the quantity of evaluation indicators or criteria. Accordingly, corresponding indicator or criteria weight vector β_k can be described as follows:

$$\begin{cases} \beta_k = (\beta_{k1}, \beta_{k2}, \beta_{k3}, \cdots \beta_{km})^T \quad k = 1, 2, 3, \cdots, r \\ \sum_{i=1}^{m} \beta_{ki} = 1 \end{cases} \tag{15}$$

The combination weighting optimization model based on minimum deviation is established and shown as follows:

$$\min W = \sum_{j=1}^{n} \sum_{k=1}^{r} \sum_{i=1}^{m} (\partial_k \beta_{ki} - \partial_j \beta_{ij})^2 s.t. \begin{cases} \sum_{k=1}^{r} \partial_k = 1 \\ \partial_k \ge 0, \; k \in [1, 2 \ldots r] \end{cases} \tag{16}$$

where W denotes the minimum weight deviation between each weighting method; $\partial_k = (\partial_1, \partial_2, \partial_3 \cdots \partial_r)$ indicates weight distribution of all weighting methods.

The optimization model above can be solved by Lagrangian function method. The derivative of ∂_k components and

Table 1 | Comparison between improved and conventional entropy methods

			Weighting results	
Number	**Distribution circumstance**	**Entropy value**	**Conventional entropy method**	**Improved entropy proposed**
1	$E_i \to 1$	(0.9999,0.9998,0.9997)	(0.167,0.333,0.500)	(0.332,0.333,0.335)
2	Discrete distribution	(0.9,0.5,0.1)	(0.067,0.333,0.600)	(0.067,0.333,0.600)

λ are used to further simplify. The Lagrangian function $L(\partial, \lambda)$ and simplification form are shown as follows:

$$\begin{cases} L(\partial, \lambda) = \sum_{j=1}^{n} \sum_{k=1}^{r} \sum_{i=1}^{m} (\partial_k \beta_{ki} - \partial_j \beta_{ij})^2 + \lambda \left(\sum_{t=1}^{r} \partial_t - 1 \right) \\ \frac{\partial L}{\partial \partial_k} = r\partial_k \sum_{i=1}^{m} \beta_{ki}^2 - \partial_1 \sum_{i=1}^{m} \beta_{1i}\beta_{ki} - \partial_2 \sum_{i=1}^{m} \beta_{2i}\beta_{ki} \\ -\partial_r \sum_{i=1}^{m} \beta_{ri}\beta_{ki} + \frac{\lambda}{2} = 0 \\ \frac{\partial L}{\partial \lambda} = \sum_{k=1}^{r} \partial_k - 1 = 0 \end{cases} \tag{17}$$

where n, r, and λ are intermediate variables during the solving process. The simplification forms are multidimensional linear equations containing $r + 1$th unknown numbers. The multidimensional linear equations have unique solution vector $\partial_k = (\partial_1, \partial_2, \partial_3 \cdots \partial_r)$ if the corresponding determinant of coefficient $|A| \neq 0$. Finally, the combination weights of evaluation indicators are obtained by weighted average method.

THE IMPROVED MULTI-OBJECTIVE PARTICLE SWARM OPTIMIZATION (IMOPSO)

The standard particle swarm optimization (PSO)

Particle swarm optimization is a stochastic search algorithm based on particle learning (Li *et al.* 2016; Laskar *et al.* 2018). In PSO, a particle is used to represent the potential solution of an optimization problem. The whole particle swarm flies in the feasible space to search for the global optimum. In a D-dimension hyper-space, the velocity vector $v_{i,D} = (\mathrm{v}_{i,1}, \mathrm{v}_{i,2}, \mathrm{v}_{i,3}, \ldots \mathrm{v}_{i,D})$ and position vector $x_{i,D} = (\mathrm{x}_{i,1}, \mathrm{x}_{i,2}, \mathrm{x}_{i,3}, \ldots \mathrm{x}_{i,D})$ are related to the ith particle $i = 1, 2, \ldots..N$, where i denotes the population size, and t represents current iteration number. After each iteration, local and global optima are selected and guide the updating direction of particles in the population. Normally, the velocity and position of each particle are first initialized by random vectors within feasible ranges. Then, the new velocities and positions of particles are updated in line with the following equations:

$$v_{i,D}^{t+1} = \omega v_{i,D}^{t} + c_1\, rand_1 (pbest_{i,D}^{t} - x_{i,D}^{t}) + c_2\, rand_2 (gbest_{i,D}^{t} - x_{i,D}^{t}) \tag{18}$$

$$x_{i,D}^{t+1} = x_{i,D}^{t} + v_{i,D}^{t+1} \tag{19}$$

where $pbest_{i,D}^{t}$ represents the personal best particle for the ith particle. $gbest_{i,D}^{t}$ is the best position that the whole swarm has found so far. ω is the inertia weight, which was introduced (Shi & Eberhart 1998) in order to enhance the exploration and exploitation capability; c_1 and c_2 are called acceleration coefficients; $rand_1$ and $rand_2$ denote random numbers uniformly distributed in the range [0, 1].

In order to solve the multi-objective optimization problem, we need to convert standard PSO into multi-objective PSO. The MOPSO was first proposed to handle multi-objective optimization problems (Coello & Lechuga 2002). The MOPSO has the characteristics of less parameters, easy operation, and fast convergence. To further enhance the search capability of MOPSO, we proposed dynamic clustering and particle mutation strategies presented as follows.

Improvement strategy

Dynamic clustering strategy (DCS)

The diversity of the population will gradually decrease in the evolutionary process, so it is easy to fall into the local optimum. To this end, the dynamic clustering strategy is introduced to strengthen search capability and diversity of the particle population (Yu *et al.* 2018). The specific operation of dynamic clustering strategy is as follows. Furthermore, to improve the search ability and convergence of the algorithm, the population is divided into several sub-populations in which particles are updated separately. The best position and velocity of particles in sub-populations are recorded, respectively:

1. Assuming that the number of sub-populations is $M(k = 1, 2, \ldots.M)$ and total L particles are assigned into each sub-population.
2. The kth particle sub-population conducts non-dominated sorting first according to mutual dominance. Then, these particles are ranked in accordance with crowding distance (Raquel & Naval 2005).
3. The kth sub-population implementing DCS will be divided into two groups. One is the high-quality group and the other is the inferior group. The quantity of particles in the high-quality group is controlled by threshold ξ. If the number

of the particle is within the threshold ξ, the particle will enter the high-quality group, otherwise it will be assigned to the inferior group. The ξ is calculated according to the following equations:

$$\xi = t_{current}/T,\ \xi = \frac{1}{1+e^{\lambda}} \tag{20}$$

$$\lambda = e^{\frac{9}{10}*\mathrm{None}} - 1 \tag{21}$$

where $t_{current}$ is current iterations. T is total iteration number. λ denotes the change rate of the ξ and *None* is times the void group searched. The design of ξ is used to provide the existence of particles in both high-quality and inferior groups.

4. The two types of groups are merged after particle update. The sub-population to implement DCS in the next generation is selected randomly in all M sub-populations.

The particle update

The particles in sub-populations without implementing DCS are updated according to the strategy in conventional MOPSO. The particles in the kth sub-population implementing DCS evolve according to the following method.

1. For the particles in the high-quality group, update method is basically the same as the standard update in MOPSO. The differences lie in that the $pbest^t_{i,D}$ and $gbest^t_{i,D}$ are replaced by personal best for the ith particle in the high-quality group and the optimal particle for kth particle sub-population, respectively.
2. The particles in the inferior group are of relatively poor quality. However, the conventional update strategy is incapable of making full use of evolution information. To this end, besides the personal best and optimal particles for the kth particle sub-population, global optimal particle is also used to provide guidance information for the evolution of the inferior particles. The specific particle velocity update equation is as follows:

$$\begin{aligned} v^{t+1}_{i,D}(wt) = {} & \omega v^t_{i,D}(wt) + c_1 rand_1(pbest^t_{i,D}(wt) - x^t_{i,D}(wt)) \\ & + c_2 rand_2(xbest^t_{i,D}(wt) - x^t_{i,D}(wt)) \\ & + c_3 rand_3(gbest^t_{i,D}(wt) - x^t_{i,D}(wt)) \end{aligned} \tag{22}$$

where $pbest^t_{i,D}(wt)$ represents personal best particle for the ith particle in the inferior group; $xbest^t_{i,D}(wt)$ denotes optimal particle in the inferior group; $gbest^t_{i,D}$ is the best particle position in the whole population. c_3 and $rand_3$ are the same as c_1 and $rand_1$.

The optimal particle selection

The external archive set (EAS) is responsible for preserving the non-dominant solutions in each iteration. If the number of non-dominant particles reaches the capacity limit of the EAS, the non-dominant particles with minimum crowding distance will be eliminated. The crowding distance is calculated by the following equation:

$$Crowd_{m,dis} = \begin{cases} \sum_{obj=1}^{K} \left(\dfrac{(Fit_{m-1,obj} - Fit_{m+1,obj})}{(Fit_{\max,obj} - Fit_{\min,obj})} \right)^2, & m \in [2, S_{ca}-1] \\ \sum_{obj=1}^{K} \left(\dfrac{(Fit_{1,obj} - Fit_{2,obj})}{(Fit_{\max,obj} - Fit_{\min,obj})} \right)^2 * 2, & \mathrm{m} = 1 \\ \sum_{obj=1}^{K} \left(\dfrac{(Fit_{S_{ca}-1,obj} - Fit_{S_{ca},obj})}{(Fit_{\max,obj} - Fit_{\min,obj})} \right)^2 * 2, & \mathrm{m} = \mathrm{S_{ca}} \end{cases} \tag{23}$$

where $Crowd_{m,dis}$ = the crowding distance of mth particle in EAS. $Fit_{m-1,obj}$, $Fit_{m,obj}$, and $Fit_{m+1,obj}$ = fitness of $m-1$, m, $m+1$th particle corresponding to the objth optimization objective, respectively. $Fit_{\max,obj}$ and $Fit_{\min,obj}$ = the best and worst fitness in the EAS.

In the process of evolution, the iteration of the continuous existence of non-dominant particles in the EAS is recorded (also referred to as 'particle age' in EAS). When selecting the global optimal particle, the selective probabilities of all non-dominant particles are calculated first. Then, the non-dominant particles with the minimum probability and maximum crowding distance are selected as $gbest^t_{i,D}$. The selective probability can be calculated by the following equation:

$$P_i = \frac{ite}{Mite} \tag{24}$$

where *ite* is 'particle age' in EAS; *Mite* is corresponding maximum 'particle age'; P_i denotes the selective probability of the ith particle.

In terms of selecting the optimal particle in high-quality and inferior groups $xbest_{i,D}^{t}$, the strategy is to compare the positions of each particle in the current group and pick the optimal one. If multiple particles exist, they will be further compared to locate the optimal particle with the largest crowding distance.

The flow chart of the proposed methodology

In this paper, we construct a framework combining the IMOPSO with MCDM model based on GCA and TOPSIS. The flow chart of the framework is demonstrated in Figure 1.

The numerical simulation

Testing function

In this section, we conduct simulation experiments to demonstrate the superiority of the proposed IMOPSO with several testing functions. The testing functions are from the ZDT and DTLZ package. The NSGAII (fast elitist non-dominated sorting genetic algorithm), MOEAD (multi-objective evolutionary algorithm based on decomposition), MOEADDE (MOEAD based on differential evolution operator), dMOPSO (multi-objective particle based on decomposition), and MOPSO (multi-objective particle swarm optimization) are selected to compare with the IMOPSO. A total of 30 independent simulations are conducted to offset randomness effect. Furthermore, the IGD and GD indicators are analyzed to evaluate the performance of IMOPSO quantitatively. The IGD is an indicator for assessing convergence and solution diversity. The GD represents the distance between the true Pareto front and Pareto front searched by IMOPSO and other rivals. The smaller the IGD and GD are, the better the convergence and distribution of the solution are. We take the ZDT1, DTLZ1, and DTLZ5 for examples. The Pareto fronts obtained by IMOPSO are shown in Figure 2. The mean and standard deviation (STD) of the IGD and GD indicators are shown in Tables 1 and 2.

From Figure 2 and Tables 2 and 3, the final solutions on the Pareto front obtained by IMOPSO are characterized by uniform distribution and strong diversity. The lower IGD and GD demonstrate that IMOPSO is closer to the true Pareto and has advantages in convergence, distribution, and diversity of solutions compared with other methods. Therefore, the IMOPSO is verified to have advantages on solution quality and stable performance compared with other methods selected.

Sensitivity analysis of parameters

In this section, simulation is conducted to analyze the sensitivity of parameters in the method proposed. The sensitivity of population size and inertia weight are analyzed, and results are shown in Tables 4 and 5 where we take the DTLZ1 testing function for instance.

Inspecting the results in Tables 4 and 5, it can be concluded that the best inertia weight is 0.90 and population size is 200. The IGD and GD indicators present a descending trend with the increase of inertia weight until the value of inertia weight is 0.9. Similarly, as the population size increases, the quality of solutions becomes better. Meanwhile, more computation time will cost as the complexity of algorithm is strongly associated with population size. Therefore, although the IGD and GD indicators are not their best when population size is 200, it will save a large amount of computation time compared with simulations under population sizes of 300 and 350. Finally, we defined the inertia weight and population size as 0.90 and 200, respectively.

CASE STUDY

Decision-making for flood control operation of Hongjiadu reservoir

In order to verify the validity and reasonability of the GCA-TOPSIS model, the flood control operation schemes of Hongjiadu reservoir were used to make the optimal decision calculation. The schemes shown in Table 6 are derived from articles by Ma *et al.* (2007) and Lu *et al.* (2015). The indicator weights are calculated and shown in Table 7 according to the proposed CWMMD.

In Table 6, the E_{power} denotes power generation; W_{aban} is the water abandoned in the reservoir; ΔZ is difference between the water level at the end of operation and the

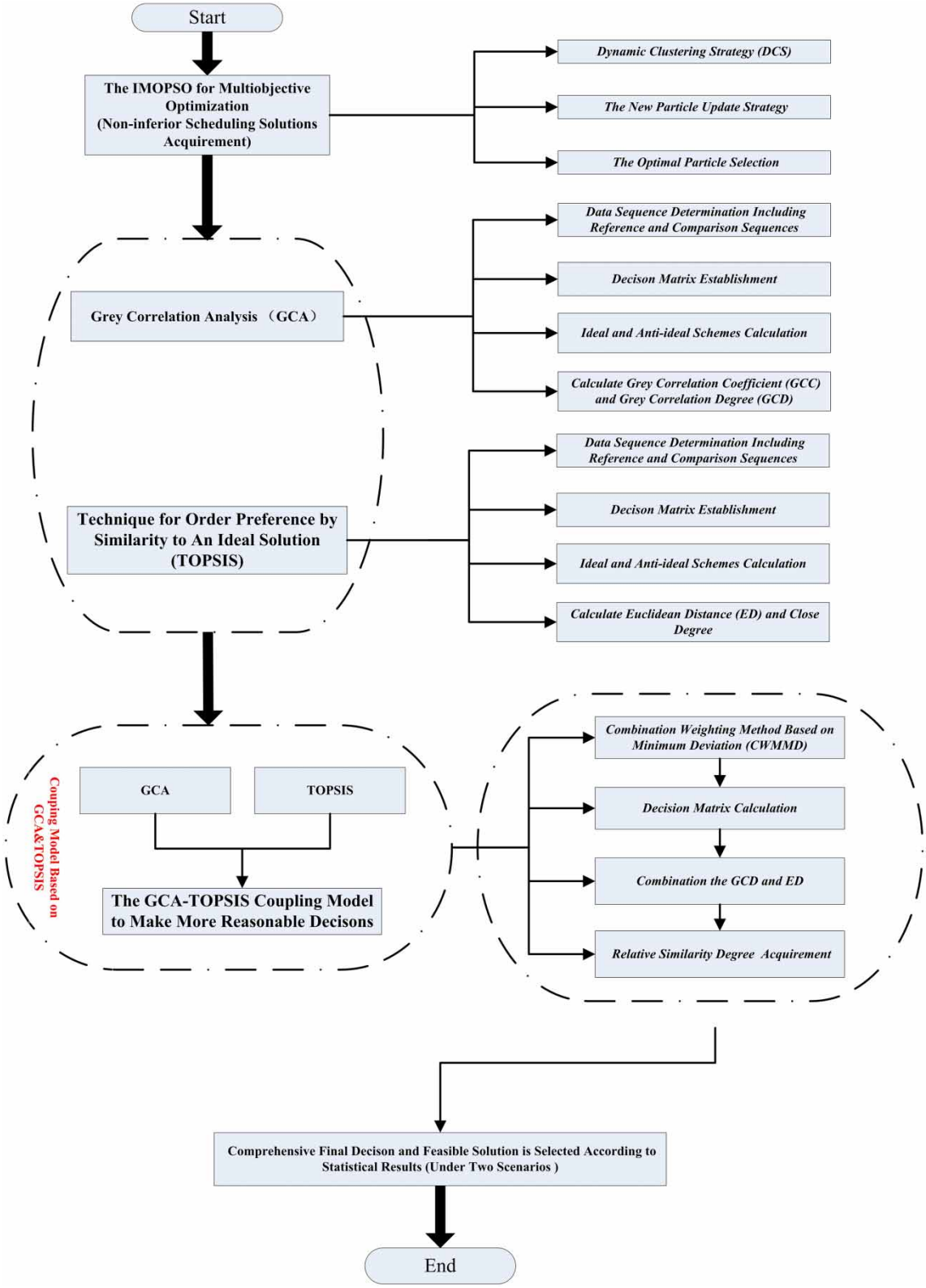

Figure 1 | The flowchart of the IMOPSO coupling with MCDM model based on GCA and TOPSIS.

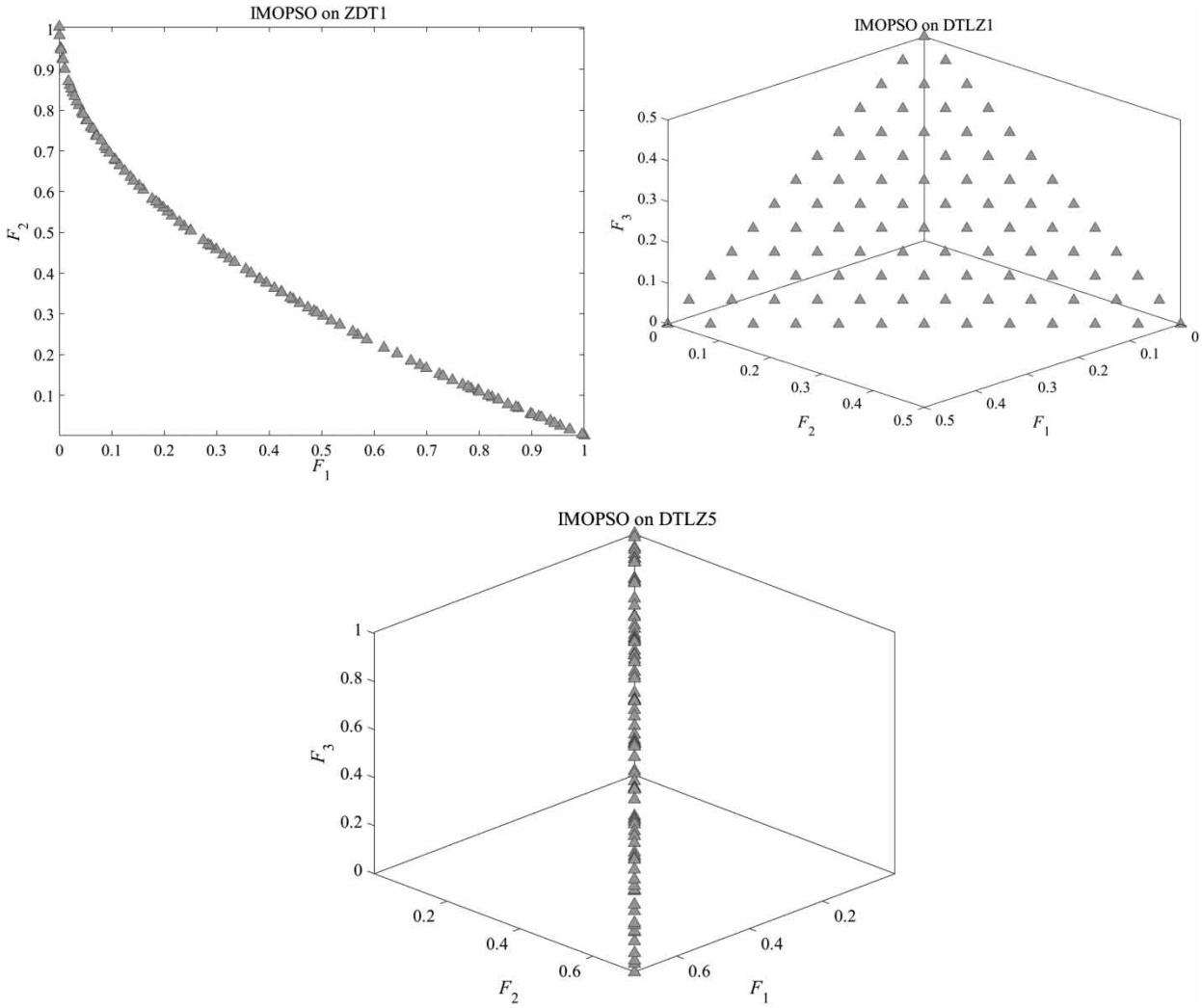

Figure 2 | The Pareto front obtained by IMOPSO.

Table 2 | The mean and standard deviation (STD) of the IGD index

Function testing	NSGAII	MOEAD	dMOPSO	MOEADDE	MOPSO	IMOPSO
	The mean of IGD					
ZDT1	2.23×10^{-2}	8.22×10^{-2}	4.37×10^{-3}	4.60×10^{-2}	2.13×10^{-2}	$\mathbf{2.63\times10^{-3}}$
DTLZ1	6.69×10^{-2}	4.11×10^{-1}	8.73×10^{-3}	7.77×10^{-2}	6.96×10^{-2}	$\mathbf{1.14\times10^{-3}}$
DTLZ5	1.77×10^{-1}	3.91×10^{-1}	1.01×10^{-2}	2.21×10^{-1}	1.58×10^{-2}	$\mathbf{1.99\times10^{-3}}$
	The STD of IGD					
ZDT1	3.06×10^{-2}	5.44×10^{-2}	1.70×10^{-3}	8.25×10^{-2}	2.75×10^{-3}	$\mathbf{2.03\times10^{-5}}$
DTLZ1	6.11×10^{-2}	1.09×10^{-1}	3.41×10^{-3}	2.16×10^{-1}	6.26×10^{-3}	$\mathbf{1.08\times10^{-5}}$
DTLZ5	1.47×10^{-1}	2.00×10^{-1}	4.13×10^{-3}	3.54×10^{-1}	1.61×10^{-3}	$\mathbf{1.88\times10^{-5}}$

Table 3 | The mean and standard deviation (STD) of the GD index

Function testing	NSGAII	MOEAD	dMOPSO	MOEADDE	MOPSO	IMOPSO
	The mean of IGD					
ZDT1	1.23×10^{-3}	2.16×10^{-2}	9.29×10^{-4}	4.44×10^{-2}	3.54×10^{-3}	$\mathbf{5.63\times10^{-5}}$
DTLZ1	3.68×10^{-3}	4.75×10^{-2}	1.81×10^{-4}	3.20×10^{-2}	4.50×10^{-3}	$\mathbf{2.76\times10^{-5}}$
DTLZ5	6.03×10^{-3}	8.17×10^{-3}	2.08×10^{-3}	1.69×10^{-1}	8.32×10^{-3}	$\mathbf{3.55\times10^{-5}}$
	The STD of GD					
ZDT1	6.67×10^{-3}	5.28×10^{-3}	7.94×10^{-4}	5.98×10^{-2}	5.09×10^{-3}	$\mathbf{4.90\times10^{-5}}$
DTLZ1	1.33×10^{-2}	1.06×10^{-2}	1.58×10^{-4}	6.72×10^{-2}	6.51×10^{-3}	$\mathbf{1.21\times10^{-6}}$
DTLZ5	1.89×10^{-2}	1.94×10^{-3}	1.92×10^{-4}	1.10×10^{-1}	1.32×10^{-2}	$\mathbf{8.53\times10^{-5}}$

Table 4 | The sensitivity of inertia weight

		The inertia weight ω						
Index	**Statistics**	**0.2**	**0.3**	**0.4**	**0.6**	**0.75**	**0.9**	**0.95**
IGD	Mean	1.42×10^{-3}	1.37×10^{-3}	1.41×10^{-3}	1.33×10^{-3}	1.19×10^{-3}	$\mathbf{1.18\times10^{-3}}$	1.20×10^{-3}
	STD	2.57×10^{-5}	2.30×10^{-5}	1.83×10^{-5}	1.39×10^{-5}	1.30×10^{-5}	$\mathbf{1.24\times10^{-5}}$	1.31×10^{-5}
GD	Mean	2.52×10^{-5}	2.68×10^{-5}	2.48×10^{-5}	2.33×10^{-5}	2.28×10^{-5}	$\mathbf{2.22\times10^{-5}}$	2.24×10^{-5}
	STD	4.09×10^{-6}	3.79×10^{-6}	3.58×10^{-6}	3.63×10^{-6}	3.43×10^{-6}	$\mathbf{3.35\times10^{-6}}$	3.44×10^{-6}

Table 5 | The sensitivity of population size

		Population size						
Index	**Statistics**	**80**	**100**	**150**	**200**	**250**	**300**	**350**
IGD	Mean	1.41×10^{-3}	1.36×10^{-3}	1.40×10^{-3}	1.18×10^{-3}	1.19×10^{-3}	1.17×10^{-3}	1.16×10^{-3}
	STD	2.04×10^{-5}	1.88×10^{-5}	1.73×10^{-5}	1.24×10^{-5}	1.33×10^{-5}	1.34×10^{-5}	1.25×10^{-5}
GD	Mean	2.39×10^{-5}	2.43×10^{-5}	2.40×10^{-5}	2.22×10^{-5}	2.25×10^{-5}	2.21×10^{-5}	2.21×10^{-5}
	STD	3.86×10^{-6}	3.58×10^{-6}	3.45×10^{-6}	3.35×10^{-6}	3.34×10^{-6}	3.35×10^{-6}	3.29×10^{-6}

Table 6 | Flood control schemes of Hongjiadu reservoir

Scheme	Description	E_{power}/10^4 kWh	W_{aban}/10^8 m^3	ΔZ/m	V_f/10^8 m^3	Q_{mout}/m^3
1	Flood pre-discharge scheduling scheme	5,451.89	3.5	0.09	1.48	2,995
2	Peak flood staggering scheme	5,445.45	3.58	0.19	1.4	3,005
3	Peak clipping scheduling scheme	5,388.15	3.78	0.3	1.32	3,193
4	Flood control schemes which adjust	5,442.58	3.57	0.25	1.44	1,935
5	opening sequence and frequency of reservoir gate in Schemes 1, 2, 3	5,447.42	3.56	0.17	1.42	3,004
6		5,421.96	3.69	0.22	1.38	3,106

Table 7 | Evaluation indicator weights of flood control

Evaluation indicator	Indicator weight		
	Improved entropy method	AHP	CWMMD
E_{power}	0.1801	0.2520	0.2169
W_{aban}	0.1803	0.2095	0.1953
ΔZ	0.2622	0.2423	0.2520
V_f	0.1807	0.1504	0.1652
Q_{mout}	0.1967	0.1458	0.1706

ideal water level; V_f is the flood control capacity used; Q_{mout} is the maximum reservoir discharge.

The GCC matrix between each scheme and the ideal and anti-ideal solution ($\varsigma^+$and ς^-) are shown in Tables 8 and 9.

The relative similarity degree C_i^* and result of scheme decision after the scheme sorting are displayed in Table 10.

Inspecting Table 10, the scheduling schemes in descending order are $1 \succ 4 \succ 5 \succ 2 \succ 6 \succ 3$. The sort order of schemes is consistent with that of Ma *et al.* (2007). However, the method in Ma *et al.* (2007) only consider the subjective indicator weight ignoring objective information. As a result, the decision-making results of this method are easily influenced by the knowledge and experience of decision-makers. On the contrary, we take fully objective and subjective information into consideration using the combination weighting method based on minimum deviation. Furthermore, the GCA contributes to reflect the uncertain information (grey information) and internal connection between multi-indicators. Meanwhile, the TOPSIS can describe the overall similarity between alternative and ideal schemes. The coupled GCA-TOPSIS makes the decision-making and scheduling scheme optimization process more reasonable and convincing through merged relative similarity degree.

Table 10 | The result of scheduling scheme decision-making using GCA-TOPSIS model

Scheduling scheme	TOP_i^+	GCA_i^+	C_i^*	Scheme sorting
1	0.5376	0.6332	0.5854	①
2	0.4514	0.5716	0.5115	④
3	0.4630	0.3612	0.4121	⑥
4	0.4722	0.5925	0.5323	②
5	0.4711	0.5852	0.5282	③
6	0.4200	0.4706	0.4453	⑤

Table 8 | The GCC matrix between each scheme and the ideal solution

Scheduling scheme	E_{power}/10^4 kWh	W_{aban}/10^8 m^3	ΔZ/m	V_f/10^8 m^3	Q_{mout}/m^3	GCC	GCC with dimensionless treatment
1	1.000	1.000	1.000	0.333	0.372	0.784	1.000
2	0.832	0.636	0.512	0.500	0.370	0.581	0.741
3	0.333	0.333	0.333	1.000	0.333	0.443	0.566
4	0.774	0.667	0.396	0.400	1.000	0.635	0.810
5	0.877	0.700	0.568	0.444	0.370	0.608	0.775
6	0.516	0.424	0.447	0.571	0.349	0.462	0.589

Table 9 | The GCC matrix between each scheme and the anti-ideal solution

Scheduling scheme	E_{power}/10^4 kWh	W_{aban}/10^8 m^3	ΔZ/m	V_f/10^8 m^3	Q_{mout}/m^3	GCC	GCC with dimensionless treatment
1	0.333	0.333	0.333	1.000	0.761	0.516	0.579
2	0.357	0.412	0.488	0.500	0.770	0.494	0.555
3	1.000	1.000	1.000	0.333	1.000	0.890	1.000
4	0.369	0.400	0.677	0.667	0.333	0.496	0.557
5	0.350	0.389	0.447	0.571	0.769	0.489	0.550
6	0.485	0.609	0.568	0.444	0.878	0.590	0.663

Table 11 | The main parameters and characteristic water levels of cascade reservoirs and power station

Characteristic water level and parameters	Cascade reservoirs in Qingjiang		
	Shuibuya	Geheyan	Gaobazhou
Normal storage water level (m)	400	200	80
Flood control level (m)	391.8	193.6	78.5
Dead water level (m)	350	160	78.09
Total storage capacity (10^8 m^3)	45.89	30.18	4.03
Beneficial reservoir capacity (10^8 m^3)	23.83	19.75	0.54
Installed capacity (MW)	1840	1212	270
Annual utilization hours of installed capacity (h)	2,450	2,533	3,563
Guaranteed output (MW)	310.0	241.0	77.3
Comprehensive efficiency coefficient	8.50	8.50	8.40
Maximum water head (m)	203.0	121.6	40.0
Minimum water head (m)	147.0	80.7	22.3
Mean water head (m)	186.6	112.0	35.4

Further comparison of the scheduling schemes shows that scheme 1 and 4 effectively utilize flood resources to increase the power generation with pre-discharge measure to control flood. Thus, the scheduling schemes 1 and 4 are optimal for the decision-maker. However, scheme 6 and 3 take more conservative measures of flood peak mitigation to hold back the flood only at the time of flood peak arrival, failing to make the best use of flood resources. Accordingly, these schemes are incompatible with the decision-maker. The decision results coincide with practical scheduling schemes for flood control in Hongjiadu reservoir.

Decision-making for multi-objective operation of Qingjiang cascade reservoirs

As presented in the above, the GCA-TOPSIS has been verified to acquire a reasonable scheduling scheme for single reservoir flood control system. For the cascade reservoirs in the basin, the formulation, evaluation, and optimization of the scheduling scheme is essentially a multi-objective, multi-attribute, and multi-turn decision-making problem in the same way. In this section, multi-objective reservoir operation in Qingjiang river is chosen as one case. The GCA-TOPSIS model is applied to take balanced consideration of multiple scheduling objectives and find the optimal scheme sort order for the decision-maker.

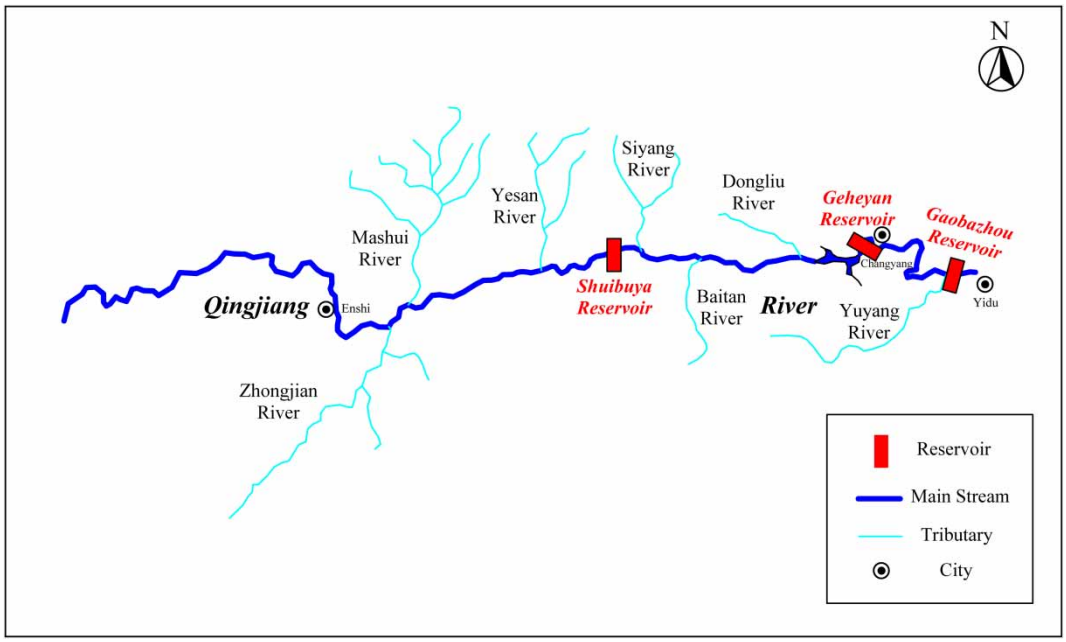

Figure 3 | Generalization of cascade reservoir system in Qingjiang river.

Overview of cascade reservoirs' system in Qingjiang river

Qingjiang river is the largest tributary of the middle Yangtze river which flows through Enshi, Badong, Changyang, and Yidu located in Hubei province. A total of three reservoirs and hydropower stations with large installed capacity, regulating storage are located on the river. The Shuibuya reservoir with multi-year regulating storage and the largest installed capacity, is the most important reservoir of the cascade development in Qingjiang river basin. The Geheyan reservoir is a huge water conservancy project with major functions of power generation and flood control, and is of navigational benefit. Gaobazhou reservoir, situated on the lower reaches of the Qingjiang river, plays an important role in the reverse regulation of upstream Geheyan (Yang *et al.* 2019b, 2019c). The main characteristic parameters of cascade reservoirs are shown in Table 11. A generalization of the cascade reservoir system in Qingjiang river basin is described in Figure 3.

Parameter selection of IMOPSO

The control parameters in IMOPSO are selected as follows with contrastive analysis. The size of EAS is defined as 30. The particle population is 200 and sub-populations assigned M are predefined as 10. Accordingly, the number of particles in each sub-population is 20. The upper and lower bound of velocity is in the interval of [−4,4]. The inertia weight ω is 0.90. The maximum iterations are defined as 500.

The scheduling scenarios

Two scheduling scenarios are proposed with the emphasis on multi-objective ecological scheduling and water supply scheduling, respectively. The specific scenarios are described as follows.

Scenario (1): Take multiple objectives including power generation, guaranteed hydropower station and ecological water spill and shortage into account. The solutions by IMOPSO are evaluated and ranked using the GCA-TOPSIS model.

Scenario (2): Take multiple objectives including power generation, water supply and ecological water spill and shortage into account. The solutions by IMOPSO are evaluated and ranked through the GCA-TOPSIS model.

RESULTS AND DISCUSSION

Scenario (1): Multi-objective ecological scheduling (MOES): For this scenario, the maximum power generation and guaranteed hydropower output and minimum ecological water shortage and spill are considered. The

Table 12 | The scheduling solution set of Qingjiang cascade reservoirs (1–30)

	Multiple objectives		
Scheme number	Power generation (10^8 kW·h)	Guaranteed hydropower output (10^4 kW)	Ecological water spill and shortage (10^8 m^3)
1	82.920	78.876	165.562
2	82.948	79.479	165.442
3	82.927	83.541	164.633
4	82.941	84.540	164.516
5	82.963	77.711	165.793
6	82.939	78.602	165.616
7	82.944	83.413	164.659
8	82.949	81.564	165.027
9	82.943	82.672	164.807
10	82.941	84.729	164.498
11	82.959	77.974	165.741
12	82.946	83.299	164.682
13	82.938	85.071	164.463
14	82.945	80.624	165.214
15	82.943	84.195	164.551
16	82.943	84.698	164.501
17	82.963	77.711	165.793
18	82.955	79.220	165.492
19	82.945	83.835	164.586
20	82.947	83.361	164.669
21	82.949	83.160	164.704
22	82.951	82.423	164.855
23	82.951	82.850	164.769
24	82.951	82.883	164.763
25	82.949	83.073	164.725
26	82.951	82.850	164.769
27	82.953	81.964	164.946
28	82.955	80.734	165.191
29	82.956	80.519	165.234
30	82.960	79.091	165.518

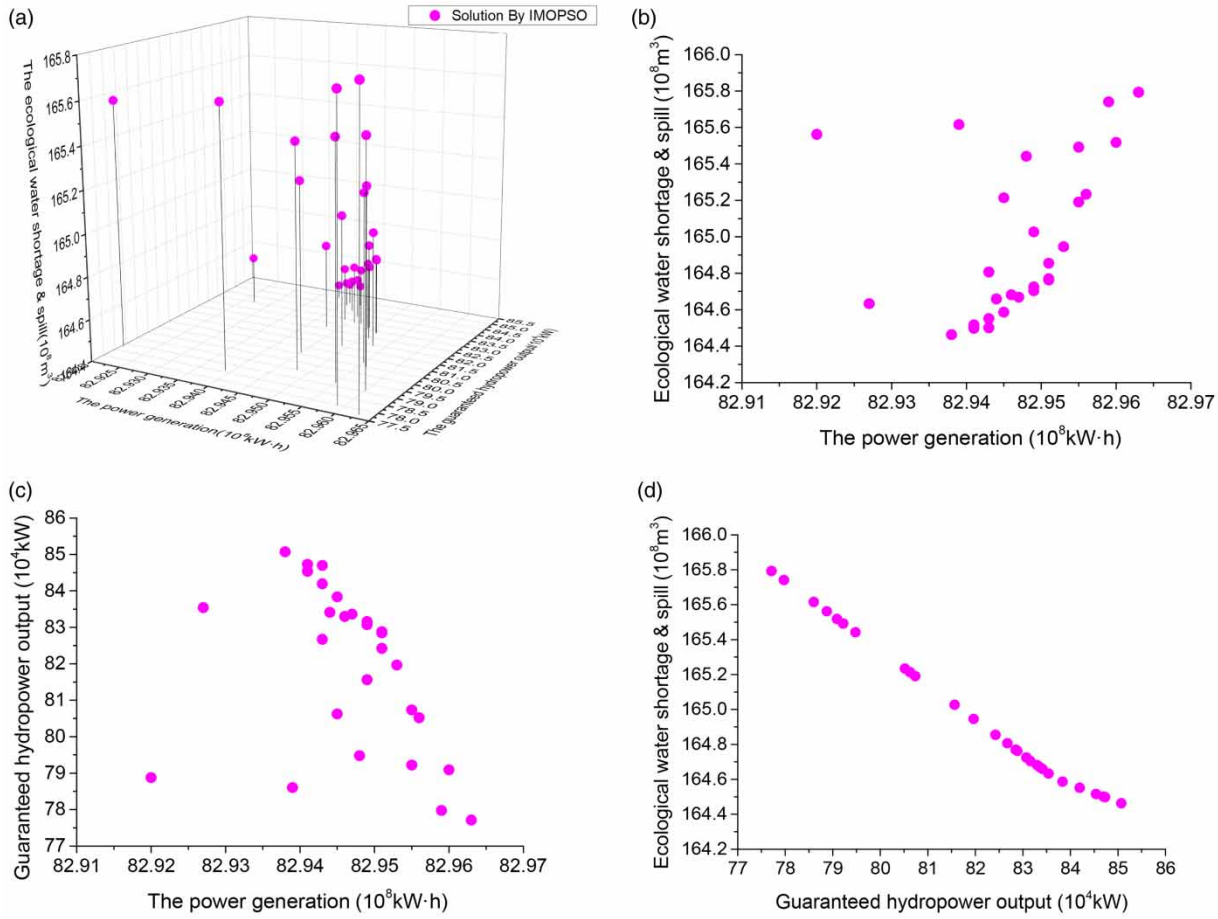

Figure 4 | The Pareto fronts between multiple objectives.

hydrologic and hydraulic constraints can be found in Zhu *et al.* (2017) and Yang *et al.* (2019b, 2019c). The details of optimization objectives are listed as follows.

1. Power generation:

$$Max\ f_1 = Max\ E_{LEC} = \max \sum_{i=1}^{G} \sum_{t=1}^{T} N_{i,t}\ \Delta t \qquad (25)$$

$$N_{i,t} = K_i Q_{i,t}^{ELC}\ H_{i,t}$$

2. Guaranteed hydropower output:

$$Max\ f_2 = Max\ N_{grt} = max\left\{ \min \sum_{i}^{G} N_{i,t} \right\} \qquad (26)$$

3. Ecological water spill and shortage:

$$Min\ f_3 = MinEco_{YS} = \min \sum_{t=1}^{T} \sum_{j=1}^{C} |Q_{j,sx}^{t} - Q_{j,eco}^{t}| \Delta t \qquad (27)$$

where E_{LEC} and Eco_{YS} = power generation and ecological water spill and shortage; Δt is scheduling interval; G and T = total amount of reservoir and scheduling intervals, respectively; C = quantity of control cross section which is matched with reservoirs; $N_{i,t}$ = power output of the ith hydropower station at tth interval; K_i = efficiency coefficient

Table 13 | The indicator weights calculated by CWMMD with emphasis on power generation and ecological benefits

	Indicator		
Decision tendency	**Power generation**	**Guaranteed hydropower output**	**Ecological water spill and shortage**
Power generation	0.5798	0.1256	0.2946
Ecological benefit	0.3059	0.0948	0.5993

of unit in the ith hydropower station; $Q_{i,t}^{ELC}$ = the power generation flow for the ith reservoir at tth interval; N_{grt} is guaranteed hydropower output of cascade reservoirs; $Q_{j,sx}^{t}$ = reservoir water release corresponding to the jth control cross section; $Q_{j,eco}^{t}$ = different level of ecological water requirements downstream of the reservoir corresponding to the jth control cross section.

For the input of the MOES model, we select one typical observed inflow process. Then, the IMOPSO is used to solve the MOES model. The optimal scheme set and Pareto fronts are demonstrated in Table 12 and Figure 4.

Inspecting Table 12 and Figure 4, the reverse and competitive relationship between the power generation, guaranteed output is presented which implies that power generation will improve with the violation of guaranteed output benefit. Moreover, power generation of cascade reservoirs and downstream ecological benefit also shows contradictoriness and opposition. However, with the increase of guaranteed output, decrease of ecological overflow and water shortage means increase of ecological benefit, and implies the compatibility between the cascade reservoir output and ecological benefits. For the decision-maker, they should select the suitable scheme from the solution sets to implement. To this end, with the GCA-TOPSIS model, we rank solution sets in accordance with power generation tendency and ecological benefit tendency, respectively. The indicator weights calculated by CWMMD are shown in Table 13. The relative similarity degree C_i^* and solution sorting results are demonstrated in Table 14.

It can be seen from Table 14 that scheme 16 and 13 are the most ideal for decision-makers when decision tendency is power generation and ecological benefit, respectively. In terms of scheme 16, the objective of power generation and guaranteed output is fully considered. Moreover, the ecological benefit obtained by this scheme outperforms most other schemes. Meanwhile, as the indicator weights calculated are 0.5798, 0.1256, and 0.2946, the decision process will place more emphasis on power generation and ecological benefit. The sorting results in Table 14 are in accordance with this principle to some extent. It should be noted that we discuss the MOES for cascade reservoirs rather than reservoir scheduling which focus on economic benefits. Therefore, scheduling schemes are not just ranked in descending order as the power generation increases. The ecological objective also has a non-negligible and significant influence on scheme evaluation and decision. On the other hand, as the decision process tends to ecological benefit, corresponding indicator weights are 0.3059, 0.0948, and 0.5993. It is evident that scheme sorting results under this situation are basically consistent with variation tendency of ecological water spill and shortage. The specific optimal

Table 14 | The relative similarity degree C_i^* and solution sorting results

	Power generation tendency		Ecological benefit tendency	
Ranking	Relative similarity degree C_i^*	Scheme number	Relative similarity degree C_i^*	Scheme number
1	0.6575	16	0.7413	13
2	0.6544	10	0.7288	10
3	0.6513	13	0.7263	16
4	0.6481	19	0.7254	4
5	0.6477	4	0.7139	15
6	0.6463	15	0.7064	3
7	0.6416	21	0.7001	19
8	0.6403	20	0.6818	7
9	0.6398	25	0.6738	20
10	0.6395	24	0.6717	12
11	0.6387	23	0.6607	21
12	0.6387	26	0.6536	25
13	0.6336	12	0.6399	24
14	0.6295	7	0.6376	23
15	0.6268	22	0.6376	26
16	0.6253	27	0.6331	9
17	0.6032	9	0.6082	22
18	0.5999	28	0.5733	27
19	0.5980	29	0.5439	8
20	0.5956	8	0.4767	28
21	0.5751	30	0.4691	14
22	0.5582	3	0.4593	29
23	0.5520	18	0.3735	2
24	0.5512	17	0.3613	1
25	0.5512	5	0.3508	18
26	0.5487	14	0.3440	30
27	0.5287	11	0.3239	6
28	0.5259	2	0.2673	11
29	0.4575	6	0.2654	17
30	0.3678	1	0.2654	5

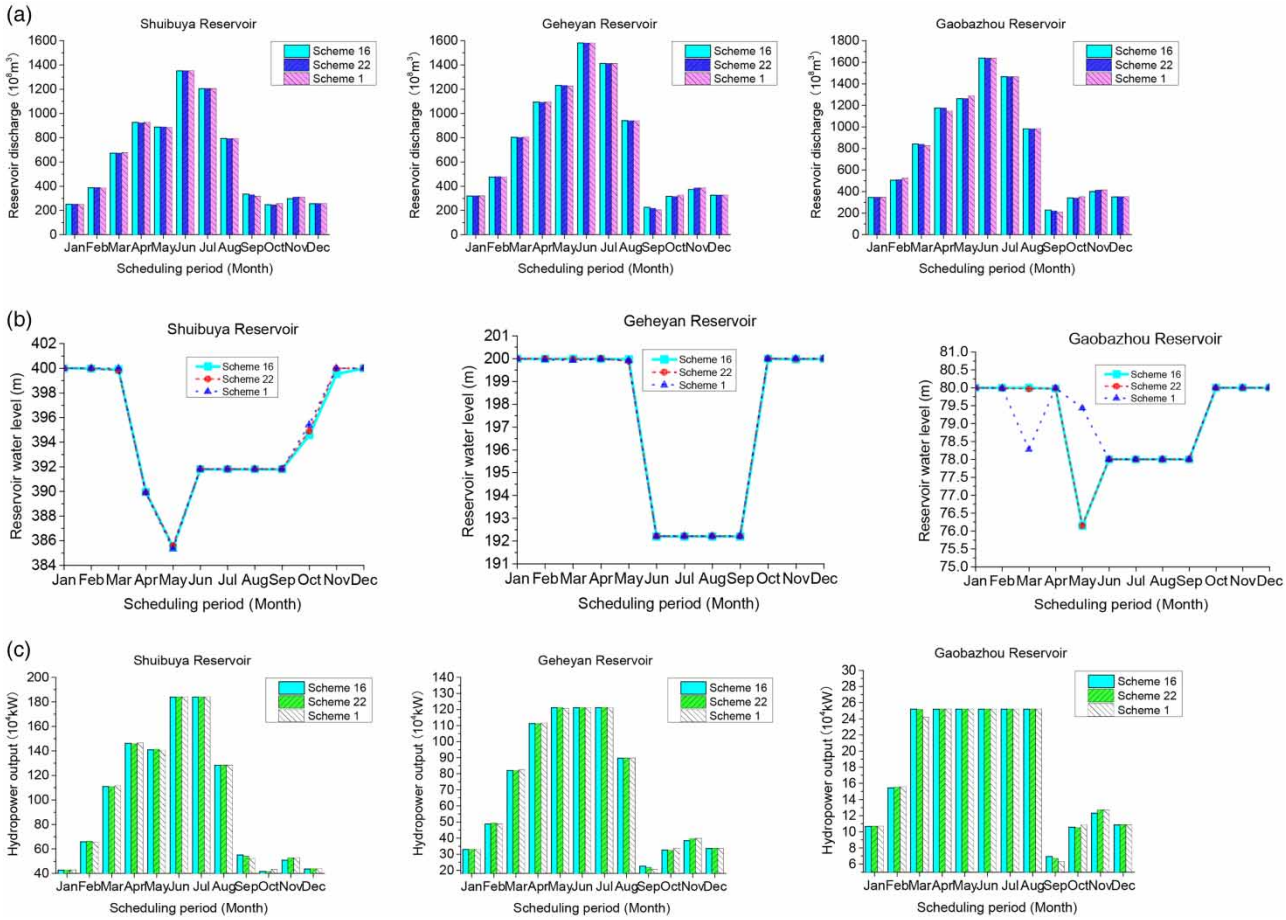

Figure 5 | The scheme comparison of MOES in Qingjiang cascade reservoirs (power generation tendency). (a) Reservoir discharge. (b) Water level process. (c) Output process.

scheduling schemes of each decision tendency are shown in Figures 5 and 6, respectively. The medium and worst schemes are added as comparison.

Due to the flood control task undertaken by Qingjiang cascade reservoirs in the flood season, the flood control benefit becomes the main factor. As a result, it can be seen from Figures 5 and 6 that the scheduling optimization space is strictly limited. Instead, the differences between schemes are mainly reflected in the dry season. Power generation efficiency requires the reservoir to operate at a high-water head, consequently, the variation range of flow rate is increased, and natural runoff will be changed, to a large extent, which produces obvious competition between power generation and ecological benefits. Meanwhile, guaranteed output benefit needs to maintain stability of power generation flow under the condition of certain amount of water. The ecological flow in dry season is simultaneously beneficial to hydropower output effect because the differences between schemes exist in this season. Therefore, the compatibility between ecological and guaranteed hydropower output benefits is remarkable.

Scheme 16 in Figure 5 places emphasis on the power generation with taking serious account of ecological benefit. Accordingly, it increases corresponding reservoir discharge in the dry season in order to protect the stability of guaranteed output and downstream ecological flow to a certain extent. As a result, the total power generation will be sacrificed which is shown in Table 12. In comparison, scheme 22 outperforms on total power generation and makes full use of high-water head effect; however, its guaranteed output is relatively lower than that of scheme 16 due to large variation of hydropower output. The large variation of output also implies instability of reservoir discharge

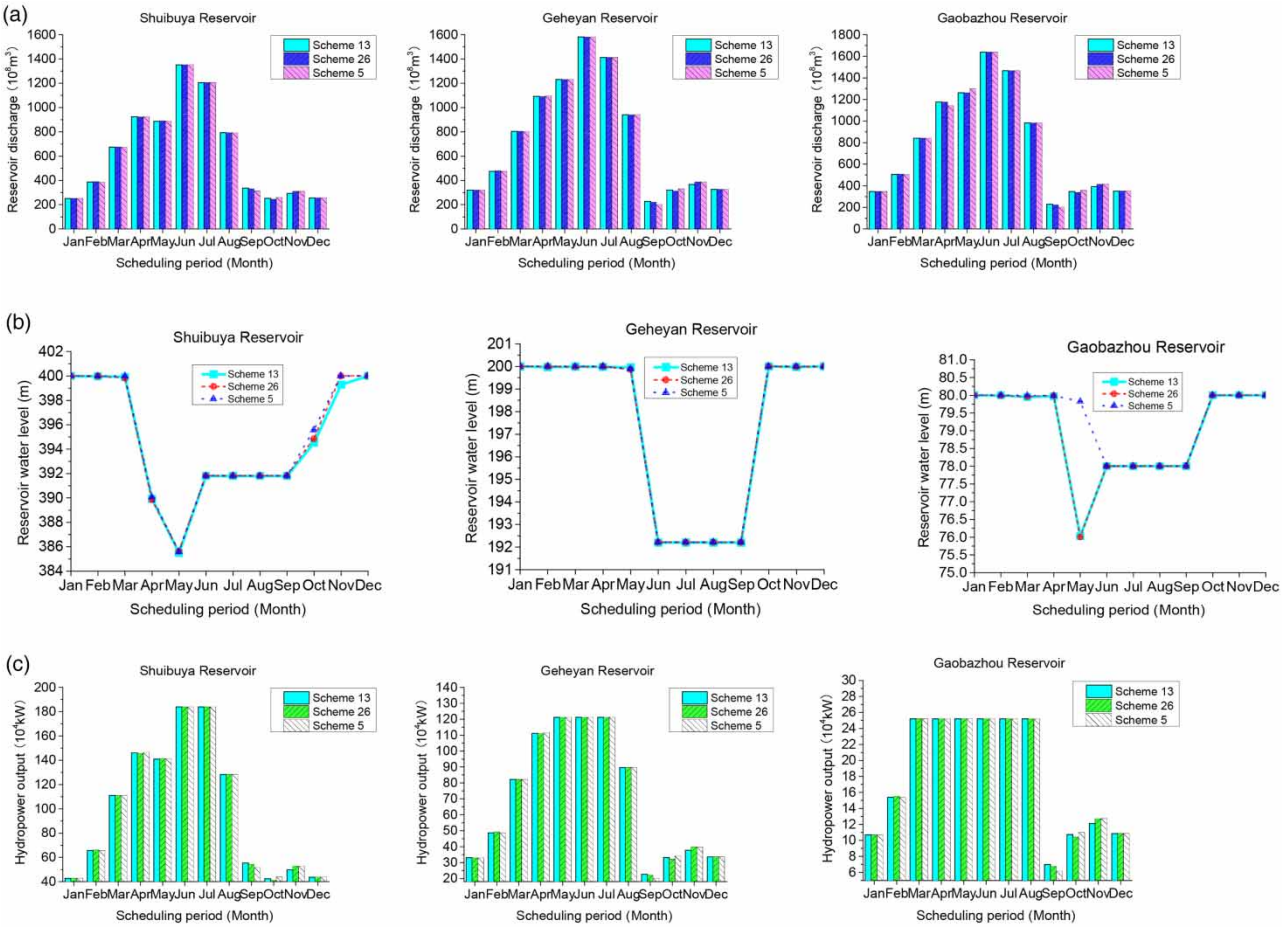

Figure 6 | The scheme comparison of MOES in Qingjiang cascade reservoirs (ecological benefit tendency). (a) Reservoir discharge. (b) Water level process. (c) Output process.

which impairs the ecological benefit. In terms of scheme 13, which tends to achieve the ecological benefit, the ecological water spill and shortage in the initial stage of the flood season is larger than other schemes. However, with a small growth rate, the total amount of ecological spill and shortage is small, and the stable variation is more beneficial to ecological benefit. In the meantime, the hydropower output is also outstanding as discharge in the flood season increases.

Scenario (2): Multi-objective water supply scheduling (MOWSS): In this scenario, optimization goals are adjusted so that the water supply benefit is added, and ecological benefit is described in the form of ecological flow guarantee rate. Similarly, the water supply guarantee rate is used for representing water supply benefit. Moreover, power generation benefit described above is also considered. The details are shown as follows.

1. Maximum average water supply guarantee rate (AWSGR):

$$Max\ f_4 = Max\ W_{SB} = max \frac{W_G}{W_D} * \frac{1}{C*T}$$
$$W_G = \sum_{t=1}^{T}\sum_{j=1}^{C} W_{gs}^{j,t}, \quad W_D = \sum_{t=1}^{T}\sum_{j=1}^{C} W_{xs}^{j,t} \tag{28}$$

2. Maximum average ecological flow guarantee rate (AEFGR):

$$Max\ f_5 = Max\ Eco = max \frac{\sum_{t=1}^{T}\sum_{j=1}^{C}(Q_{j,sx}^{t}/Q_{j,eco}^{t})\Delta t}{T*C} \tag{29}$$

where W_{SB} = the water supply guarantee rate, which is the ratio of volume of water supply W_G to water demand W_D. $W_{gs}^{j,t}$ = the water delivered to jth control section at the tth interval. Similarly, $W_{xs}^{j,t}$ = water demand for

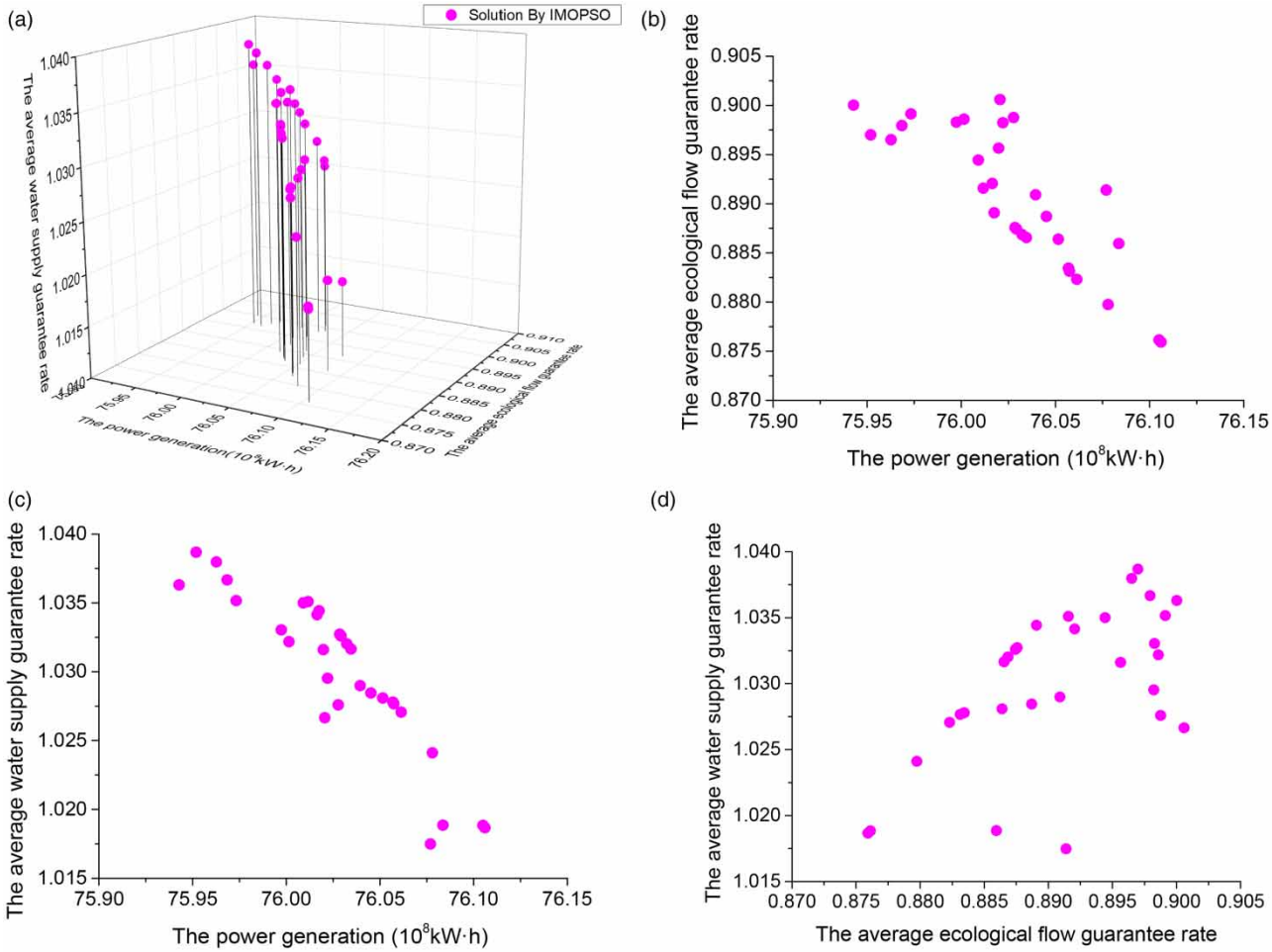

Figure 7 | The Pareto fronts between multiple objectives.

the jth control section at the tth interval. Eco = ecological water supply guarantee rate which is described as the ratio of $Q^t_{j,sx}$ to $Q^t_{j,eco}$.

Similarly, the IMOPSO is applied to solve the MOWSS model and the corresponding Pareto front of the non-inferior scheduling scheme is demonstrated in Figure 7.

It can be seen from Figure 7 that mutual competition and contradiction between the power generation and water supply and ecological flow guarantee rates is evident. Accordingly, improving power generation will bring about the violation of water supply and ecological benefits and vice versa. However, with the increase of AWSGR, the AEFGR also increases which implies the mutual compatibility and promotion between water supply and ecological benefits. This may be explained by the increase of AWSGR needs larger reservoir discharge, which is also beneficial for maintaining downstream ecological health. However, some solutions in Figure 7(d) present contradictory relation which can be attributed to the fact that the water diversion task may directly transport reservoir water to users. As a result, it will bring about an adverse effect on power generation and ecological benefits.

Furthermore, the GCA-TOPSIS model is used to evaluate and rank scheduling schemes obtained by IMOPSO.

Table 15 | The indicator weights calculated by CWMMD with emphasis on water supply ecological benefit

	Indicator		
Decision tendency	**Power generation**	**AEFGR**	**AWSGR**
Water supply	0.2703	0.1043	0.6254

The indicator weights shown in Table 15 are calculated in the same way used in Scenario (1). The scheme evaluation and sorting results are listed in Table 16. The optimal scheduling scheme is shown in Figure 8. The medium and worst schemes are used as a comparison.

Table 16 shows that scheme 2 is the most ideal one for the decision-maker. In terms of scheme 2, the objective of AWSGR is optimum in comparison with other schemes.

Table 16 | The relative similarity degree C_i^* and solution sorting results

	Water supply tendency	
Ranking	**Relative similarity degree C_i^***	**Scheme number**
1	0.6391	2
2	0.6372	3
3	0.6207	4
4	0.6143	9
5	0.6129	12
6	0.6002	15
7	0.6002	5
8	0.5994	13
9	0.5880	1
10	0.5799	7
11	0.5740	16
12	0.5719	19
13	0.5687	8
14	0.5639	14
15	0.5628	17
16	0.5572	21
17	0.5365	10
18	0.5225	18
19	0.5132	20
20	0.5090	11
21	0.5072	22
22	0.5003	23
23	0.4979	25
24	0.4952	6
25	0.4890	26
26	0.4471	27
27	0.3765	29
28	0.3744	30
29	0.3662	28
30	0.3404	24

As the indicator weights calculated are 0.2703, 0.1043, and 0.6254, the decision process tends to place more emphasis on water supply benefit. The sorting results are in accordance with the quality of the objective of AWSGR. In other words, the scheme with the larger AWSGR is better than others. Thus, the sorting result of the optimal scheme to that of the worst scheme is basically consistent with the variation trend of water supply guarantee rate.

As can be seen from Figure 8, the scheduling space is limited during the flood control season, while differences are mainly reflected in the dry season. Scheme 2 increases reservoir discharge and produces water stage drawdown to guarantee the water supply task during the dry season. Meanwhile, the larger quantity of water discharge is beneficial to alleviate ecological water shortage at the dry season stage. Thus, the compatibility relationship between water supply and ecological protection is presented. On the other hand, although the hydropower output outperforms other schemes in the initial stage of the dry season, high-water head is not efficiently utilized to guarantee total power generation. In terms of scheme 24, it focuses more energy on the power generation benefit. To this end, reservoir water discharge is cut down to operate at higher-water head and concentrate drawdown before the arrival of the flood season. As a result, high-water head effect is fully used to play the power generation benefit. However, the smaller discharge in the early stage of the dry period will alleviate the benefit of AWSGR and AEFGR, and great fluctuation of reservoir discharge is harmful to maintain stability of water supply and ecological health.

In short, the decision-making method of GCA-TOPSIS has shown strong applicability in solving the MCDM problem of multi-objective reservoir ecological and water supply operation. It can quickly and reasonably select the most ideal scheme of comprehensive benefits under different decision-making scenarios for the reservoir decision-makers.

CONCLUSION

In this paper, we propose a framework including IMOPSO for non-inferior solutions' acquirement, the MCDM model based on grey correlation analysis (GCA) and the multi-attribute method of TOPSIS. In terms of the MCDM model, the

Figure 8 | The scheme comparison of MOWSS in Qingjiang cascade reservoirs (water supply benefit tendency). (a) Reservoir discharge. (b) Water level process. (c) Output process.

GCA contributes to reflecting the difference between the change trend in the scheduling scheme sets and ideal scheme, while the TOPSIS can reflect the overall similarity between alternative and ideal schemes. The combination of GCA and TOPSIS can take uncertainty factors and grey characteristics in the multi-objective decision process fully into account, and accurately describe the comprehensive quality of alternative scheduling schemes.

The GCA-TOPSIS is applied to MCDM, including multi-objective flood control operation of Hongjiadu reservoir, and ecological and water supply operation of Qingjiang cascade reservoirs. Based on scheduling schemes obtained by IMOPSO and combination weighting of evaluation indicators calculated by CWMMD, GCA-TOPSIS can effectively evaluate and select the most ideal scheme of comprehensive benefits under different decision-making scenarios for the reservoir decision-makers. In summary, the decision-making method of GCA-TOPSIS shows strong applicability in solving the evaluation of multi-objective flood control, ecological and water supply scheduling schemes. The rationality of the decision result is also illustrated and verified, which implies that the decision-making method GCA-TOPSIS can provide strong theoretical support for the implementation of multi-objective balanced scheduling decisions in complex reservoir systems.

ACKNOWLEDGEMENTS

This work is supported by the Research and Extension Project of Hydraulic Science and Technology in Shanxi Province 'Study on the Key Technology for Joint Optimal

Operation of Complex Multi-Reservoir System and Water Network' (2017DSW02), the Science and Technology Project of Yunnan Water Resources Department 'Comprehensive Water Saving and Unconventional Water Utilization Research', the National Key Basic Research Program of China (973 Program) (2012CB417006), the National Science Support Plan Project of China (2009BAC56B03). The first author was supported by a fellowship from the China Scholarship Council for his visit to the IIHR-Hydroscience and Engineering, University of Iowa, C. Maxwell Stanley Hydraulics Laboratory, Iowa City, USA.

REFERENCES

Abo-Sinna, M. A., Amer, A. H. & Ibrahim, A. S. 2008 Extensions of TOPSIS for large scale multi-objective non-linear programming problems with block angular structure. *Applied Mathematical Modelling* **32** (3), 292–302.

Afshar, A., Marino, M. A., Saadatpour, M. & Afshar, A. 2011 Fuzzy TOPSIS multi-criteria decision analysis applied to Karun reservoirs system. *Water Resources Management* **25** (2), 545–563.

Azamathulla, H. M., Wu, F. C., Ghani, A. A., Narulkar, S. M., Zakaria, N. A. & Chang, C. K. 2008 Comparison between genetic algorithm and linear programming approach for real time operation. *Journal of Hydro-Environment Research* **2** (3), 172–181.

Chen, S. Y. & Lu, C. C. 2015 Assessing the competitiveness of insurance corporations using fuzzy correlation analysis and improved fuzzy modified TOPSIS. *Expert Systems* **32** (3), 392–404.

Coello, C. A. & Lechuga, M. S. 2002 MOPSO: A proposal for multiple objective particle swarm optimization. *Proceedings of the Congress on Evolutionary Computation, Honolulu, HI, USA* **2**, 1051–1056.

Dai, C., Wang, Y. & Ye, M. 2015 A new multi-objective particle swarm optimization algorithm based on decomposition. *Information Sciences* **325** (3), 541–557.

Deng, H., Yeh, C. H. & Willis, R. J. 2000 Inter-company comparison using modified TOPSIS with objective weights. *Computer & Operations Research* **27** (4), 963–973.

He, Y. Y., Xu, Q. F., Yang, S. L. & Liao, L. 2014 Reservoir flood control operation based on chaotic particle swarm optimization algorithm. *Applied Mathematical Modelling* **38** (17–18), 4480–4492. https://doi.org/10.1016/j.apm.2014.02.030.

Hwang, C. & Yoon, K. 1981 *Multiple Attribute Decision Making: Methods and Applications*. Springer, Berlin, Germany.

Jia, B. Y., Simonovic, S. P., Zhong, P. A. & Yu, Z. B. 2016 A multi-objective best compromise decision model for real-time flood mitigation operations of multi-reservoir system. *Water Resources Management* **30**, 3363–3387. https://doi.org/10.1007/s11269-016-1356-0.

Jiang, W., Liang, J. R. & Jiang, J. B. 2007 Multi-objective Vague decision making based on gray connection analysis. *Computer Engineering and Applications* **43** (18), 171–173.

Karimi, M., Moztarzadeh, F. & Pakzad, A. 2012 Application of Fuzzy TOPSIS for Group Decision Making in Evaluating Financial Risk Management. In: *2012 International Conference on Innovation Management and Technology Research (ICIMTR 2012)*, Malacca, Malaysia, pp. 215–218.

Laskar, N. M., Guha, K., Chatterjee, I., Chanda, S., Baishnab, K. L. & Paul, P. K. 2018 HWPSO: A new hybrid whale-particle swarm optimization algorithm and its application in electronic design optimization problems. *Applied Intelligence* **2**, 533–542.

Lei, X. P., Robin, Q. & Liu, Y. 2016 Evaluation of regional land use performance based on entropy TOPSIS model and diagnosis of its obstacle factors. *Transactions of the Chinese Society of Agricultural Engineering* **32** (13), 243–253.

Li, Q. Q. & Ouyang, S. 2015 Research on multi-objective joint optimal flood control model for cascade reservoirs in river basin system. *Natural Hazards* **77** (3), 2097–2115.

Li, Y. H., Zhou, J. Z., Zhang, Y. C., Liu, L. & Qin, H. 2009 Risk decision model for the optimal operation of reservoir flood control and its application. *Water Power* **35** (4), 19–22.

Li, L., Liu, F., Long, G. Z., Guo, P. S. & Bie, X. F. 2016 Modified particle swarm optimization for BMDS interceptor resource planning. *Applied Intelligence* **44** (3), 471–488.

Lu, Y. L., Chen, J. S., Qi, J., Ji, P. & Zhou, J. Z. 2015 Multi-objective decision making method for reservoir flood operation based on improved entropy weight and set pair analysis. *Water Resources and Power* **33** (1), 43–46.

Luo, J., Chen, C. & Xie, J. C. 2015 Multi-objective immune algorithm with preference-based selection for reservoir flood control operation. *Water Resources Management* **29**, 1447–1466.

Ma, Z. P., Chen, S. L. & Li, X. Y. 2007 Application of grey relation decision to flood control of multipurpose reservoir. *Journal of China Three Gorges University (Natural Science)* **29** (4), 289–291.

Malekmohammadi, B., Zahraie, B. & Kerachian, R. 2011 Ranking solutions of multi-objective reservoir operation optimization models using multi-criteria decision analysis. *Expert Systems With Applications* **38** (6), 7851–7863. https://doi.org/10.1016/j.eswa.2010.12.119.

Peng, A. B., Peng, Y., Zhou, H. C. & Zhang, C. 2015 Multi-reservoir joint operating rule in inter-basin water transfer-supply project. *Science China Technological Sciences* **58** (1), 123–137.

Raquel, C. R. & Naval, P. C. 2005 An effective use of crowding distance in multiobjective particle swarm optimization. In: *Genetic and Evolutionary Computation Conference*, Washington, DC, USA. doi: 10.1145/1068009.1068047.

Sheikholeslami, F. & Navimipour, N. J. 2017 Service allocation in the cloud environments using multi-objective particle swarm optimization algorithm based on crowding distance. *Swarm and Evolutionary Computation* **35**, 53–64.

Shi, Y. & Eberhart, R. 1998 A modified particle swarm optimizer. In: *IEEE International Conference on Evolutionary Computation Proceedings. IEEE World Congress on Computational Intelligence IEEE*, pp. 69–73.

Shi, J. Y., Xue, F., Li, Y. J., Yang, T., Gong, Y., Ma, L. & Ling, L. T. 2017 Active distribution system planning for low-carbon objective using immune binary firefly algorithm. *Journal of Tianjin University (Science and Technology)* **50** (5), 507–513. doi:10.11784/tdxbz201605082.

Wang, Z. X. & Wang, Y. Y. 2014 Evaluation of the provincial competitiveness of the Chinese high-tech industry using an improved TOPSIS method. *Expert Systems with Applications* **41** (6), 2824–2831.

Wang, H. X., Chu, J. G., Zhang, C. & Zhou, H. C. 2014 Identifying the key water levels in reservoir operation on ecological objectives. *Water Science and Techology: Water Supply* **14** (6), 1160–1167.

Yang, Z., Yang, K., Su Lyu, W. & Hu, H. 2019a Two-dimensional grey cloud clustering-fuzzy entropy comprehensive assessment model for river health evaluation. *Human and Ecological Risk Assessment: An International Journal* doi: 10.1080/10807039.2018.1536519.

Yang, Z., Yang, K., Hu, H. & Su Lyu, W. 2019b The cascade reservoirs multi-objective ecological operation optimization considering different ecological flow demand. *Water Resources Management* **33** (1), 207–228. https://doi.org/10.1007/s11269-018-2097-z.

Yang, Z., Yang, K., Su Lyu, W. & Hu, H. 2019c The multi-objective operation for cascade reservoirs using MMOSFLA with emphasis on power generation and ecological benefit. *Journal of Hydroinformatics* **21** (2), 257–278. doi: https://doi.org/10.2166/hydro.2019.064.

Yu, Y., Liang, L., Jiang, Y. J. & Du, S. F. 2004 A new modified approach of TOPSIS based on fuzzy preference. *Systems Engineering* **8** (22), 87–90.

Yu, H., Wang, Y. J., Chen, Q. & Xiao, S. L. 2018 Multi-objective particle swarm optimization based on multi-population dynamic cooperation. *Electronic Science and Technology* **31** (1), 1–6.

Zain, M. Z. B. M., Kanesan, J., Chuah, J. H., Saroja, D. & Graham, K. 2018 A multi-objective particle swarm optimization algorithm based on dynamic boundary search for constrained optimization. *Applied Soft Computing* **70** (3), 680–700.

Zeng, Y. H., Jiang, T. B. & Quan, X. Z. 2003 Application of grey system theory to selection of reservoir's normal water level. *Hydropower Automation and Dam Monitoring* **27** (1), 57–59.

Zhang, J. & Liang, C. 2009 Application of TOPSIS model based on gray correlation coefficient matrix in the evaluation of water environmental quality. *Journal of Sichuan University (Engineering Science Edition)* **41** (4), 97–101.

Zhu, F. L., Zhong, P. A., Xu, B., Wu, Y. N. & Zhang, Y. 2016 A multi-criteria decision-making model dealing with correlation among criteria for reservoir flood control operation. *Journal of Hydroinformatics* **18** (3), 531–543. https://doi.org/10.2166/hydro.2015.055.

Zhu, F. L., Zhong, P. A., Sun, Y. M. & Yeh, W. W.-G. 2017 Real-time optimal flood control decision making and risk propagation under multiple uncertainties. *Water Resources Research* **53**, 10635–10654.

First received 28 February 2019; accepted in revised form 24 May 2019. Available online 21 June 2019